

Enhancement performance of rough solar air heater having circular wire ribs

Yashoda nand tiwari ¹, Dr. Pankaj Jain ²

¹ M. Tech. Research Scholar, Assistant Professor

Department of School of Energy and Environment Management.
UIT, RGPV, Bhopal, India

Abstract : The objective of this paper to study of heat and fluid flow processes in an artificially roughened solar air heater. Artificially roughness introduce under side of absorber plate of solar air heater in the form of small transverse wire ribs. Solar air heater is a type of heat exchanger, which convert solar radiation into thermal (heat) energy. Thermal performance of solar air heater has been found very low due to low convective heat transfer coefficient from the absorber plate to the air. Use of artificially roughness is an effective technique to enhance the rate of heat transfer. This investigation performed on circular section with different values of Reynold numbers range from 3800-18000. Reynold no, relative pitch height (p/e) and relative roughness height (e/d) are chosen as design variables. Two-dimensional CFD simulation is perform using the ANSYS FLUENT version 12.1 .The renormalization group (RNG) k-e model is selected as the most appropriate once. Comparing the results obtain by our study of CFD approach of circular sections with different rib pitch (p) and roughness heights (e) of Reynold number range 3800-18000. The effect of pitch, rib height, relative roughness height (e/D), relative roughness pitch (p/e) on Nusselt number and friction factor have been discussed and the result compared with rough duct and smooth duct under simpler flow conditions. Nusselt enhancement factor and friction enhancement factor of roughed solar air heater have been optimized the considering the thermo-hydraulic performance. Maximum Thermo-hydraulic performance have been found 1.72 of circular transverse wire rib section at $p=10$ mm, $e=1.4$ mm, and $e/D=0.042$. Hence, these values are chose best design dimensions of circular section.

Keywords: rough solar air heater, rib pitch, rib height, relative roughness height, Reynold no, nusselt no, friction factor, thermal enhancement factor.

1. Introduction

Presently, the world's papulation is nearly 7.5 billion and projected are a global papulation approximate 10 billion by mid-century. Due to growing world papulation and increasing modernization, global energy demand is projected to more than double during the first half of the twenty-first century and to more than triple by end of 21st century. Fulfil future energy demand can either conventional resources or non-conventional resources of energy, but conventional fossil fuel energy use has had serious and growing negative environmental impacts, such as CO₂ emissions, global warming, air pollution, deforestation, and overall global environmental degradation. Additionally, fossil fuel reserves are not infinite or renewable. Other hand renewable energy fulfil sufficient supplies of clean and sustainable energy for the future is the global society's most daunting challenge for the twenty-first century. The future will be a mix of energy technologies with renewable sources such as solar, wind, and biomass playing an increasingly important role in the new global energy economy. If the twenty-first century sustainable energy challenge is not met quickly, many less-developed countries will suffer major famines and social instability from rising energy prices. Ultimately, the world's economic order is at stake.

Fossil fuels, which are, still the main source of energy, which are exhausting rapidly. Thus to meet this continuously increasing demand of energy, we have to use alternative or renewable source of energy some commonly used renewable energy source are sun, wind, sea, geothermal and biomass. These sources are almost inexhaustible and are replenish by natural porous. Further, there use does not cause of environmental population. Sun's energy can be utilize as thermal and photovoltaic. Wind energy, which is air in motion is caused by to mains factors-first is the heating and cooling of atmosphere which generates convection currents. Heating is cause by the absorption of solar energy on the earth's surfaces and in the atmosphere. Secondly is the rotation of earth with respect to atmosphere and its motion around the sun. Due to virtue of their motion, are the potential source of energy. Gravitational force of heavenly bodies like sun and moon causes periodic rise & fall in sea water level, which is known as tides. Geothermal energy or heat of the earth is the thermal energy found within the rocks in earth's crust. Source of this thermal energy are magnetic & radioactive decay processer occur within the interior of the earth. Organic matter produced by plants and their derivatives is called biomass. In India where agriculture is still main occupation of most of villagers, Bio-thermal energy is a very important source of energy.

Solar energy, which is the primary sources of all kind of energy on the earth, originates in the sun as results of thermonuclear fusion reaction. The sun is the most significant sources of renewable energy because sun is more than 100 times larger than the earth. The sun is made of two gasses, hydrogen (H) and helium (He). Solar energy is generate due to fusion of reaction in which hydrogen is always turning into helium, in an enormous explosion, which liberate huge amount of energy. This energy is radiated by the sun in the form of electromagnetic radiations. Solar power reaching at the top of the atmosphere is about 10^{17} watts and that on earth's surface is 10^{16} watts, while total power requirement of the world is 10^{13} watts. So, if we can use only 5% of this energy, it will be 50 times more than the requirement. Generation of solar energy from sun is based on the principle of Einstien equation. i. e. $E=mc^2$, where E is energy, m is mass and c is velocity of light. Solar energy has been used since prehistoric times, but in a most primitive manner. Before 1970, some research and development was carried out in a few countries to exploit solar energy more efficiently, but most of this work remained mainly academic. After the dramatic rise in oil prices in the 1970s, several countries began to formulate extensive research and development programmers to exploit solar energy.

Solar air heater is one of the basic equipment through which solar energy is converted into thermal energy. Solar air heaters, because of their simple designing, are cheap and most widely used as a collection devices of solar energy. The main applications of solar air heater are space-heating, seasoning of timber, curing of industrial products and these can be effectively used for curing/drying of concrete/clay building components. A conventional solar air heater generally consists of an absorber plate, a rear plate, insulation below the rear plate, transparent cover on the exposed side, and the air flows between the absorbing plate and rear plate. A solar air heater is simple in design and requires little maintenance. However, the value of the heat transfer coefficient between the absorber plate and air is low and this result in lower efficiency. For this reason, the surfaces are sometime rough in the airflow passage.

The use of artificial roughness on a surface is an effective technique to enhance the rate of heat transfer to fluid flowing in a duct. Artificial roughness in the form of repeated ribs has been found to be a convenient method to enhance the rate of heat transfer. Ribs of various shapes and orientations have been employed and the performance of such system has been investigated. Artificial roughness has been used to enhance the heat transfer coefficient by creating turbulence in the flow. However, it would also result in an increase in friction losses and hence greater pumping power requirements for air through the duct. In order to keep the friction losses at a low level, the turbulence must be created only in the region very close to the duct surface, i.e. in the laminar sub-layer.

The concept of artificial roughness was first applied by Joule [1] to enhance heat transfer coefficients for in-tube condensation of steam and since then many experimental investigations were carried out on the application of artificial roughness in the areas of

cooling of gas turbine, electronic equipment's nuclear reactors, and compact heat exchangers etc. Nunner [2] was the first who developed a flow model and likened this model to the temperature profile in smooth tube flow at increased Prandtl number. Prasad and Mullick [3] were the first who introduced the application of artificial roughness in the form of small diameter wire attached on the underside of absorber plate to improve the thermal performance of solar air heater for drying purposes. After Prasad and Mullick's [4] work, a number of experimental investigations on solar air heater involving roughness elements of different shapes, sizes and orientations with respect to flow direction have been carried out in order to obtain an optimum arrangement of roughness element geometry [5-7]. Saini and Verma [8] conducted an experimental investigation on fluid flow and heat transfer characteristics of solar air heater duct having dimple-shaped artificial roughness. Authors found maximum value of Nusselt number corresponds to relative roughness height (e/D) of 0.0379 and relative roughness pitch (P/e) of 10. Authors also found minimum value of friction factor correspond to relative roughness height (e/D) of 0.0289 and relative pitch (P/e) of 10. Singh et al. [9] experimentally investigated the heat transfer characteristics of rectangular duct having its one broad wall heated and roughened with periodic 'discrete V-down rib'. Authors found maximum value of Nusselt number and friction factor corresponds to relative roughness pitch (P/e) of 8. Tanda [10] experimentally investigated the heat transfer coefficients and friction factors for a rectangular channel having one wall roughened having angled continuous ribs, transverse continuous and broken ribs, and discrete V-shaped ribs. Author reported that roughening the heat transfer surface by transverse broken ribs appeared to be the most promising enhancement technique for investigated rib geometries. Bhagoria et al. [11] performed experiments to determine the effect of relative roughness pitch, relative roughness height and wedge angle on the heat transfer and friction factor in a solar air heater roughened duct having wedge shaped rib roughness. Authors found maximum enhancement of Nusselt number up to 2.4 times while the friction factor up to 5.3 times for the range of parameters investigated.

Number of experimental studies have been carried out to evaluate performance of solar air heater, but very few attempts of CFD investigations have been made. Chaube et al. [12] performed a CFD analysis of heat transfer enhancement and flow characteristics due to artificial roughness in the form of ribs on a heated wall of a rectangular duct of a solar air heater for turbulent flow. A 2-D analysis of heat transfer and fluid flow through a rectangular duct with ten different rib shapes viz. rectangular, square, chamfered, triangular, etc., provided on a heated wall was carried out using commercially available CFD software, FLUENT 6.1. Shear stress transport k-u turbulence model was selected by comparing the predictions of different turbulence models with experimental results available in the literature. Kumar and Saini [13] carried out CFD based analysis of fluid flow and heat transfer characteristics of a solar air heaters having roughened duct provided with artificial roughness in arc shaped geometry. The heat transfer and flow analysis of the chosen roughness element were carried out using 3-D models. The ribs were provided on the absorber plate whereas other sides of the duct were kept smooth. FLUENT commercial CFD code was used for simulation. Different Turbulent Models namely Shear stress transport k-u, Standard k- ϵ , Renormalization group (RNG) k- ϵ and Realizable k- ϵ were tested for smooth duct having same cross-section of roughened duct in order to find out the validity of the models. Sharma and Thakur [14] conducted a CFD study to investigate the heat transfer and friction loss characteristics in a solar air heater having attachments of V-shaped ribs roughness at 60 relative to flow direction pointing downstream on underside of the absorber plate. For validating the accuracy of numerical solutions, the computations of fully developed turbulent flow forced convection in a smooth rectangular duct was carried out to compare with the exact solution for the Nusselt number and friction factor, respectively. Gandhi and Singh [15] conducted a CFD study to investigate the effect of artificial surface roughness on flow through a rectangular duct having bottom wall roughened with repeated transverse ribs of wedge shaped cross-section. Two-dimensional numerical modeling of the duct flow using FLUENT showed reasonably good agreement with the experimental observations except for the friction factor. Numerical results obtained by commercial computational fluid dynamics (CFD) code FLUENT were compared with the experimental results. Recently Yadav and Bhagoria [16] presented a detailed literature survey about different CFD investigations on artificially roughened solar air heater. Authors also reported that the results obtained by

Renormalization group (RNG) $k-\epsilon$ model were in good agreement with the Dittus Boelter and Blasius empirical correlation. In the present work a numerical investigation

of turbulent forced convection in a two-dimensional duct of a solar air heater with small diameter of transverse wire rib on the absorber plate is conducted. The upper wall is subjected to a uniform heat flux condition while the lower wall is insulated. The ribs are provided on the underside of the absorber plate whereas other sides of the duct are kept smooth. The results of the present CFD analysis have been compared with available experimental results. The main aims of the present CFD analysis are.

1. To investigate the effect of roughness height, roughness pitch, relative roughness pitch and relative roughness height on heat transfer and flow friction and
2. To find out the optimal rib dimension and arrangement in term of thermal enhancement factor.

To the best of authors' knowledge no such type of comprehensive numerical work exists in the open literature on solar air heater having small diameter of transverse wire rib roughness on the absorber plate.

2. CFD simulation and Methodology

In this section a 2-dimensional CFD simulation of artificially roughened solar air heater is investigated. Commercial CFD simulation code FLUENT (version 12.1) is used to solve the conservation equations for mass, momentum and energy. The physical model and the computational procedure are presented in the following sub-sections. The following assumptions are imposed for the computational analysis.

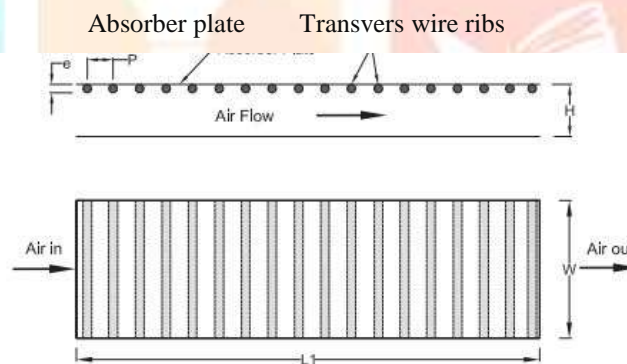


Fig.2.1 rough absorber plate having circular wire ribs

1. The flow is steady, fully developed, turbulent and two-dimensional.
2. The thermal conductivity of the duct wall, absorber plate and roughness material are independent of temperature.
3. The duct wall, absorber plate and roughness material are homogeneous and isotropic.
4. The working fluid (air) is assumed to be incompressible for operating range of solar air heaters since variation in density is very less.
5. No-slip boundary condition is assigned to the walls in contact with the fluid in the model.
6. Negligible radiation heat transfer and other heat losses.

2.1. Solution domain

The 2-dimensional solution domain used for CFD analysis has been generated as shown in Fig.2.1. The solution domain is a horizontal duct with circular transverse wire rib roughness on the absorber plate at the underside of the top of the duct while other sides

are considered as smooth surfaces. In the present analysis, a similar flow domain used for the predictions has been selected as per the details given by Chaube et al. Complete duct geometry is divided into three sections, namely, entrance section, test section and exit section. A short entrance length is chosen because for a roughened duct, the thermally fully developed flow is established in a short length 2-3 times of hydraulic diameter. The exit section is used after the test section in order to reduce the end effect in the test section. For the turbulent flow regime, ASHRAE Standard 93-2003 recommends entrance and exit length of $5\sqrt{WH}$ and $2.5\sqrt{WH}$ respectively. The top wall consists of a 0.5 mm thick absorber plate made up of aluminum. Artificial roughness in the form of small diameter galvanized iron (G.I) wires is considered at the underside of the top of the duct on the absorber plate to have roughened surface, running perpendicular to the flow direction while other sides are considered as smooth surfaces. The minimum rib height, 0.7 mm has been chosen so that the laminar sub-layer is of the same order as of roughness height at the lower flow Reynolds number. The maximum rib height is set to 1.4 mm so that the fin and flow passage blockage effects may be negligible. A uniform heat flux of 1000 w/m² is considered for computational analysis. The geometrical parameters for artificially roughened solar air heater are listed in Table 1. The operating parameters employed in this computational investigation are listed in Table 2. All dimensions is mm.

Table-1. Geometric parameters of the artificially rough solar air heater.

L1	L2	L3	W	H	D	e(mm)	P(mm)
225	115	120	100	20	33.33	0.7,1,1.4	10,15,20,25

2.2. Grid generation

Meshing of the domain is done using ANSYS ICEM CFD V12.1 software. A non-uniform mesh with very fine mesh size is used to resolve the laminar sub-layer and is shown in Fig.2.2. Since low Reynolds number turbulence models are employed, the grids are generated so as to be very fine. Present non-uniform quadrilateral mesh contained 161,568 quad cells with non-uniform quad grid of 0.24 mm cell size. This size is suitable to resolve the laminar sublayer. For grid independence test, the number of cells are varied from 103,231 to 197,977 in five steps. It is found that after 161,568 cells, further increase in cells has less than 1% variation in Nusselt number and friction factor value which is taken as criterion for grid independence.

Table-2 values of chosen operating parameters for CFD analysis

Operating parameters	Range of values
Uniform heat flux (q)	1000 w/m ²
Reynold number (Re)	3800-18000
Prandtl number (pr)	0.744
Relative roughness pitch (p/e)	7.14-35.71
Relative roughness height (e/D)	0.021-0.042
Duct aspect ratio (W/H)	5

Table-3 Thermo-physical properties of working fluid (air) and absorber plate (aluminum) for CFD analysis.

Properties	Working fluid (air)	Absorber plate (aluminum)
Density (kg/m ³)	1.225	2719

Specific heat (j/kg k)	1006	870
Viscosity (N/m ²)	1.789e-05	-
Thermal conductivity (W/m K)	0.0242	202.4

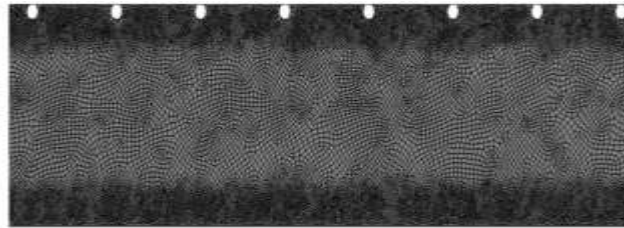


Fig-2.2 two-dimensional non-uniform mesh for circular ribs.

2.3. Governing equation

The flow phenomenon in artificially roughened solar air heater duct is governed by the steady 2-dimensional form of the continuity, the time-independent incompressible Navier-stokes equations and the energy equation. In the Cartesian tensor system these equations can be written as:

Continuity equation:

Mass balance equation is given by

Rate of increase of mass in fluid element = Net rate of flow of mass element in to fluid element

$$\frac{\partial \rho}{\partial t} + \text{div}(\rho \mathbf{u}) = 0 \quad (1)$$

This is unsteady, 3D mass conservation or continuity equation in compressible fluid.

For incompressible fluid it is given by,

$$\text{Div}(\mathbf{u}) = 0 \quad (2)$$

$$\text{or } \frac{\partial u}{\partial x} + \frac{\partial v}{\partial y} + \frac{\partial w}{\partial z} = 0$$

Momentum conservation

Rate of increase of momentum = Sum of forces

$$\frac{\partial(\rho \vec{v})}{\partial t} + \nabla \cdot (\rho \vec{v} \vec{v}) = \rho \mathbf{g} - \nabla P + \nabla \cdot (\vec{\tau}) \quad (3)$$

Energy conservation

Rate of increase of energy = Net heat added + Net rate of work done

$$\frac{\partial(\rho E)}{\partial t} + \nabla \cdot (\vec{v}(\rho E + p)) = \nabla \cdot (k_{\text{eff}} \nabla T + (\vec{\tau}_{\text{eff}} \cdot \vec{v})) \quad (4)$$

Where,

$$E = h - \frac{p}{\rho} + \frac{v^2}{2}$$

Navier Stokes Equation

$$\begin{aligned}\rho \frac{Du}{Dt} &= -\frac{\partial p}{\partial x} + \frac{\partial}{\partial x} [2\mu \frac{\partial u}{\partial x} + \lambda \text{div} u] + \frac{\partial}{\partial y} [\mu (\frac{\partial u}{\partial y} + \frac{\partial v}{\partial x})] + \frac{\partial}{\partial z} [\mu (\frac{\partial u}{\partial z} + \frac{\partial w}{\partial x})] + S_{mx} \\ \rho \frac{Dv}{Dt} &= -\frac{\partial p}{\partial y} + \frac{\partial}{\partial y} [2\mu \frac{\partial v}{\partial y} + \lambda \text{div} u] + \frac{\partial}{\partial x} [\mu (\frac{\partial u}{\partial y} + \frac{\partial v}{\partial x})] + \frac{\partial}{\partial z} [\mu (\frac{\partial v}{\partial z} + \frac{\partial w}{\partial y})] + S_{my} \\ \rho \frac{Dw}{Dt} &= -\frac{\partial p}{\partial z} + \frac{\partial}{\partial z} [2\mu \frac{\partial w}{\partial z} + \lambda \text{div} u] + \frac{\partial}{\partial x} [\mu (\frac{\partial u}{\partial y} + \frac{\partial w}{\partial x})] + \frac{\partial}{\partial y} [\mu (\frac{\partial v}{\partial z} + \frac{\partial w}{\partial y})] + S_{mz}. \quad (5)\end{aligned}$$

2.4. Boundary condition

The solution domain of the considered 2D, rectangular duct flow is geometrically quite simple. It is a rectangle on the x-y plane, enclosed by the inlet, outlet and wall boundaries.

The working fluid in all cases is air. The properties of the working fluid (air) and absorber plate material (aluminum) have been assume to remain constant at average bulk temperature. The thermo-physical properties of working fluid and absorber plate are illustrate in Table 3. No-slip conditions for velocity in solid surfaces are assume and the turbulence kinetic energy is set to zero on all solid walls. The top wall boundary condition is select as constant heat flux of 1000 W/m² and bottom wall is assume to be in adiabatic condition. A uniform air velocity is introduce at the inlet while a pressure outlet condition is apply at the exit. The Reynolds number varies from 3800 to 18,000 at the inlet. The mean inlet velocity of the flow is calculated using Reynolds number. Constant velocity of air is assume in the flow direction. The temperature of air inside the duct is also take as 300 K at the beginning. At the exit, a pressure outlet boundary condition is specified with a fixed pressure of 1.013×10^5 Pa.

2.5. Selection and validation of the model

No universal turbulence model exists that caters for all ranges of flow, laminar or turbulent. The choice of turbulence model is not only dictate by the type of flow but also by the availability of computational power and the accuracy desired. The selection and validation of turbulence model is carried out by comparing the Nusselt number predicted by different turbulence models such as Standard k-ε model, Renormalization-group k-ε model, Realizable k-ε model, Standard k-ω and Shear stress transport k-ω model with empirical correlation available for smooth duct of a solar air heater i.e. Dittus-Boelter correlation.

$$\text{Dittus-Boelter equation: } \text{Nus} = 0.023 \text{Re}^{0.8} \text{Pr}^{0.4} \quad (6)$$

Fig.2.3 compares the variation of Nusselt number with Reynolds number using different turbulence models and results obtained from Dittus-Boelter empirical correlation for a smooth duct of a solar air heater. For low Reynolds number (relevant in solar air heater), it has been observe that the results obtained by Renormalization-group (RNG) k-ε model are in good agreement with the Dittus-Boelter empirical correlation results. This ensures the accuracy of the numerical data obtained from the present work. The absolute percentage deviation of the Nusselt number data by RNG k-ε model is $\pm 2.58\%$ from the values predicted by Eq. (6). Prediction by standard k-u model shows more deviation with empirical correlation. The predictions with the standard k-u model and the SST k-u model are over-predict in comparison with Dittus-Boelter empirical correlation results whereas Standard k-ε model and Realizable k-ε model are under-predicted

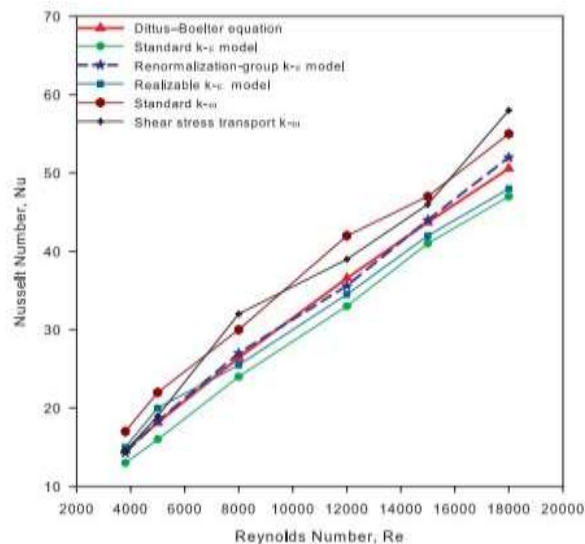


Fig -2.3 selection best model

In the present numerical study Renormalization-group (RNG) k-ε model has been selected to simulate the heat transfer and fluid flow characteristic on the basis of its closer results to the Dittus-Boelter empirical correlation result.

2.6. Solution method

In the present simulation governing equations of continuity, momentum and energy are solve by the finite volume method in the steady-state regime. The numerical method used in this study is a segregated solution algorithm with a finite volume-based technique. The governing equations are solve using the commercial CFD code, ANSYS Fluent 12.1. A second-order upwind scheme is chose for energy and momentum equations. The SIMPLE algorithm (semi-implicit method for pressure link equations) is chose as scheme to couple pressure and velocity. The convergence criteria of 10^{-3} for the residuals of the continuity equation, 10^{-6} for the residuals of the velocity components and 10^{-6} for the residuals of the energy are assumed. A uniform air velocity is introduce at the inlet while pressure outlet condition is apply at the outlet. Adiabatic boundary condition has been implement over the bottom duct wall while constant heat flux condition is apply to the upper duct wall of test section.

3. Data reduction for thermo-hydraulic performance of an artificially roughened solar air heater

Three parameters of interest for the present case are: 1. Nusselt number 2. Friction factor, and 3. Thermal enhancement factor.

Performance of any system represents the degree of utilization of input to the system. It is required to analyze thermal and hydraulic performance of a solar air heater for making an efficient design of such type of a system. Thermal performance concerns with heat transfer process within the collector and hydraulic performance concerns with pressure drop in the duct.

Average Nusselt number is defined as

$$Nu_r = hD/k \quad (7)$$

where h is convective heat transfer co-efficient.

The friction factor is computed by pressure drop, across the length of test section, and can be obtained by

$$f = \left(\frac{\Delta P}{L}\right) \frac{D}{2\rho V^2} \quad (8)$$

It is desirable that design of solar air heater should be made in such a way that it should transfer maximum heat energy to the flowing fluid with minimum consumption of pumping power. Therefore in order to analyze overall performance of a solar air heater, thermo-hydraulic performance should be evaluated by considering thermal and hydraulic characteristics of the collector simultaneously. An important performance evaluation parameter which is used to compare the heat transfer of artificially roughened duct to that of a smooth duct under constant pumping power constraint as defined by Webb and Eckert.

$$\text{Thermal enhancement factor} = \frac{Nu/Nu_s}{(f/f_s)^{\frac{1}{3}}} \quad (9)$$

where Nu_s represents Nusselt number for smooth duct of a solar air heater and can be obtained by Eq. (6) and f_s represent friction factor for smooth duct of a solar air heater and can be obtained by Blasius equation.

$$f_s = 0.0791 Re^{-0.25} \quad (10)$$

A value of this parameter greater than unity ensures the effectiveness of using an enhancement device and can be use to compare the performance of number of arrangements to decide the best among these.

4. Result and discussion

The effects of various flow and roughness parameters on the heat transfer and friction characteristics for flow of air in a roughened rectangular duct are present below. The results have been compared with those obtained in case of smooth duct operating under similar operating conditions to discuss the enhancement of heat transfer and friction factor on account of artificial roughness.

4.1 Effect of rib pitch (p)

Figs.4.1 (a) and 4.1 (b) show the variation of average Nusselt number and friction factor as a function of Reynolds number for different values of rib pitch. Distance between two successive ribs can be define as the pitch and it has great importance in heat transfer enhancement. It can be seen that the Nusselt number values is directly proposanally to Reynold number. i.e. Nu_{Nusselt} number increase with increase of Reynolds number, whereas the friction factor is inversely proposanally to Reynold number. i.e. Friction factor decreases with the increase of Reynolds number. Fig. 4.1(b) shows that the Nusselt number decreases with increasing values of the rib pitch. Fig 4.1(b) also shows that the friction factor decreases with an increase in rib pitch.

4.2 Effect of rib height (e)

Figs. 4.2(a) and 4.2(b) show the variation of average Nusselt number and friction factor as a function of Reynolds number for different values of rib height.

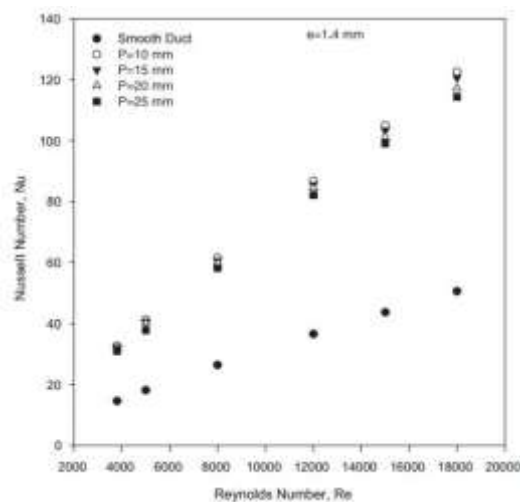


Fig-4.1(a) Effect of pitch on Nusselt no

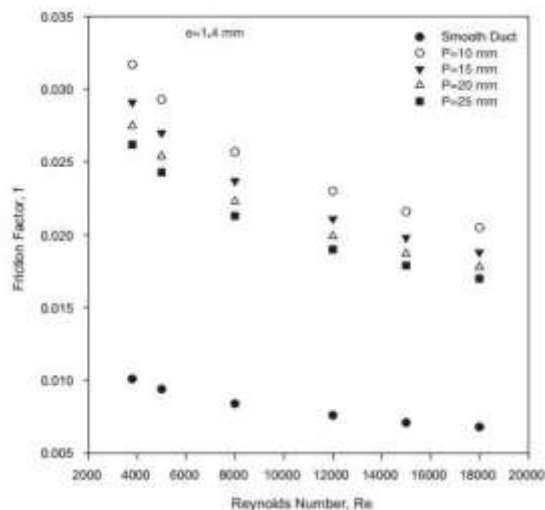


Fig-4.1(b) Effect of pitch on friction factor

It can be seen that the Nusselt number increases with the increase of Reynolds number, whereas the friction factor decreases with the increase of Reynolds number. It can also be observe from these figures that the enhancement in heat transfer of the roughened duct with respect to the smooth duct also increases with an increase in Reynolds number whereas enhancement in friction factor of the roughened duct with respect to the smooth duct also decreases with an increase in Reynolds number. Fig 7.2(a) also shows that the Nusselt number increases with increasing values of the rib height. Fig 7.2(b) also shows that the friction factor increases with increasing values of the rib height This is due to the fact that increasing value of roughness height attributed to more interruptions in the flow path. The maximum rib height is set to 1.4 mm so that the fin and flow passage blockage effects may be negligible. The height of the rib, $e = 1.4$ mm is also limited by the friction penalty during CFD simulation

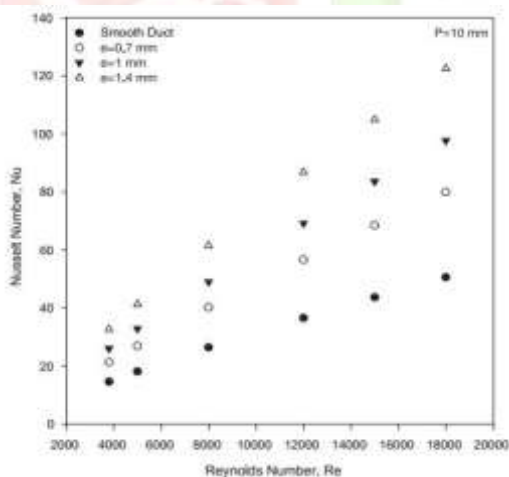


Fig-4.2(a) Effect of rib hieght on nusselt no with reynold no

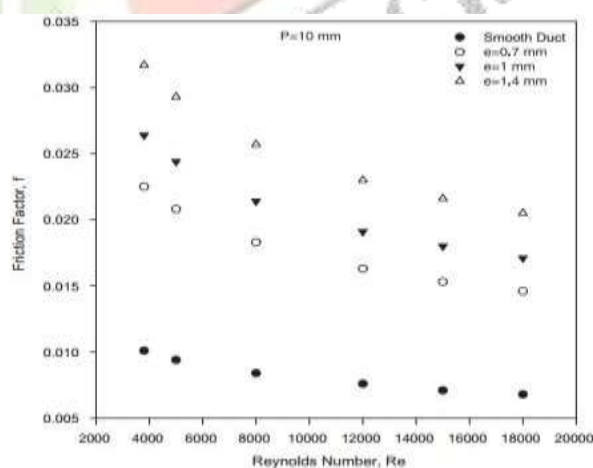


Fig-4.2(b) Effect of rib hieght on friction factor with

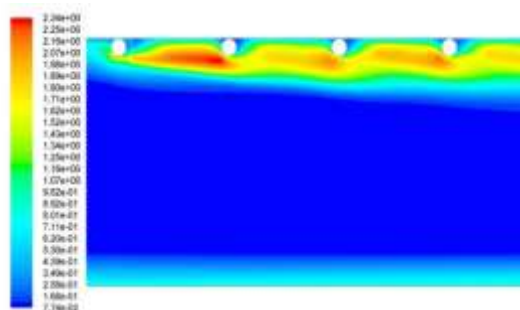


Fig-4.2(c) contour plot of kinetic energy for circular ribs.

4.3 Effect of relative roughness pitch (P/e)

Effect of the relative roughness pitch (P/e) on heat transfer has been shown typically in Figs. 4.3(a) Shows that the Nusselt number increases with increasing values of the Reynolds number in all cases as expected. It can be seen that the Fig. 4.3(a) shows the plots of Nusselt number as a function of relative roughness pitch (P/e) for different values of Reynolds number and for fixed $e/D = 0.042$ in terms of dimensionless number

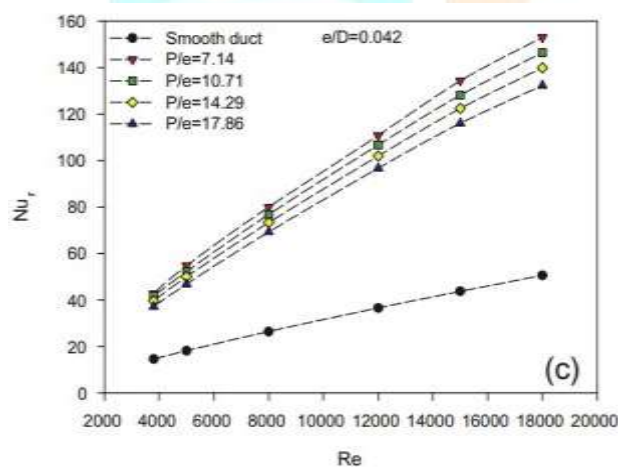


Fig-4.3(a) Effect of relative roughness pitch on nusselt no with Reynold

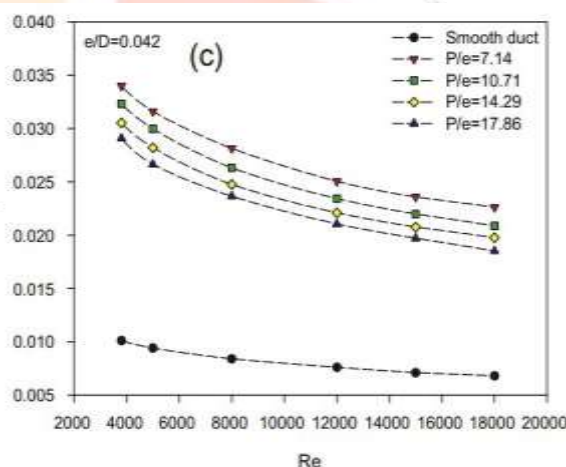


Fig-4.3(b) Effect of relative roughness pitch on friction factor on

It is seen that for a given relative roughness pitch the Nusselt number increases with decrease of relative roughness pitch. Effect of the relative roughness pitch (P/e) on friction factor has been shown in Fig 4.3(b) Fig shows that the friction factor decreases with the increasing values of the Reynolds number in all cases as expected because of the suppression of laminar sub-layer for fully developed turbulent flow in the duct. It can also be seen that friction factor values decrease with the increase in relative roughness pitch (P/e) for fixed value of relative roughness height (e/D), attributed to less number of interruptions in the flow path.

4.4 Effect of relative rib height (e/D)

Effect of relative roughness height (e/D) Figs. 4.4(a) show the effect of relative roughness height (e/D) on the heat transfer performance. It is also seen that Nusselt number increases with increase in relative roughness height (e/D) and has been found maximum corresponding to relative roughness height of 0.042. This is due to the fact that heat transfer coefficient is low at the leading edge of the circular wire rib and high at the trailing edge. Higher relative roughness height produced more reattachment of free shear layer which

creates the strong secondary flow. Hence, the heat transfer increases with the increase in relative roughness height and maximum occurs at e/D of 0.042. Fig. 4.4(a) shows the plots of Nusselt number as a function of relative roughness height (e/D) for different values of Reynolds number and for fixed $P/e=14.29$. It is seen that for a given relative roughness pitch the Nusselt number increases with an increase of relative height and increases with increasing values of the Reynolds number in all cases as expected. Effect of the relative roughness height (e/D) on the friction factor has been shown typically in Fig 4.4(b). From Fig.4.4(b) it can be seen that friction factor decreases with the increase in Reynolds number for different values of relative roughness height (e/D), because of the suppression of laminar sub-layer for fully developed turbulent flow in the duct. It is also seen that Nusselt number increases with increase in relative roughness height (e/D) and has been found maximum corresponding to relative roughness height of 0.042. Fig. shows the plots of friction factor as a function of relative roughness height (e/D) for different values of Reynolds number and for fixed $P/e=14.29$. It is seen that for a given relative roughness pitch the friction factor increases with an increase of relative height with Reynolds number for all cases as expected. Both the average Nusselt number and friction factor increases with increasing value of relative roughness height. These results broadly agree with previous experimental results reported by Verma and Prasad and Prasad and saini.

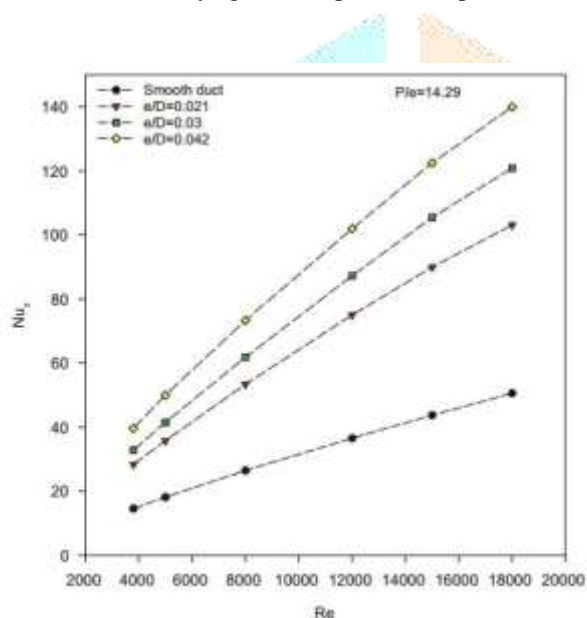


Fig-4.4(a) Effect of relative rib height on nusselt no

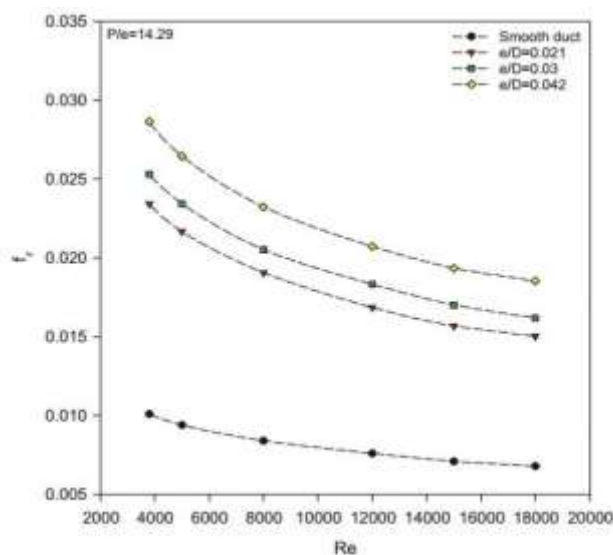


Fig-4.4 (b) Effect of friction factor with relative rib height

The effect pitch, rib height, relative roughness height (e/D) and relative pitch (P/e) with different Reynolds numbers on the heat transfer and friction characteristics for flow of air in a roughened rectangular duct are presented below in the form of tables. 4.1 & 4.2. The results have been compare with those obtained in case of smooth ducts and artificial roughness ducts under similar operating conditions.

Table:-4.1 Nusselt number enhancement factor for circular section.

D=33.33mm				Nu_r/Nu_s					
e(mm)	e/D	P(mm)	p/e	Re =3800	Re =5000	Re =8000	Re =12000	Re =15000	Re =18000
0.7	0.020	10	14.30	1.45	1.47	1.50	1.55	1.56	1.57
		15	21.42	1.43	1.45	1.18	1.51	1.54	1.55
		20	28.56	1.41	1.43	1.46	1.49	1.51	1.54
		25	35.70	1.41	1.42	1.45	1.48	1.51	1.52
1.0	0.03	10	10	1.77	1.80	1.84	1.88	1.90	1.92
		15	15	1.74	1.77	1.81	1.85	1.87	1.90
		20	20	1.73	1.75	1.80	1.83	1.86	1.87
		25	25	1.71	1.73	1.78	1.81	1.83	1.85

1.4	0.042	10	7.15	2.22	2.26	2.27	2.28	2.29	2.30
		15	10.70	2.20	2.22	2.24	2.25	2.30	2.31
		20	14.30	2.17	2.20	2.22	2.23	2.25	2.24
		25	17.87	2.12	2.15	2.18	2.20	2.21	2.18

Table:-4.2 Nusselt number enhancement factor for equilateral triangle

D=33.33mm				f_{r_r}/f_{r_s}					
e(m m)	e/D	p(mm)	p/e	Re =3800	Re =5000	Re =8000	Re =1200 0	Re =150 00	Re =180 00
0.7	0.020	10	14.30	2.21	2.20	2.16	2.13	2.14	2.13
		15	21.42	2.04	2.03	2.01	1.97	1.98	1.97
		20	28.56	1.92	1.91	1.88	1.86	1.88	1.85
		25	35.70	1.84	1.82	1.80	1.77	1.78	1.76
1.0	0.030	10	10	2.62	2.60	2.53	2.52	2.54	2.52
		15	15	2.40	2.38	2.33	2.31	2.33	2.30
		20	20	2.26	2.24	2.20	2.17	2.19	2.16
		25	25	2.16	2.14	2.10	2.07	2.10	2.07
1.4	0.042	10	7.15	3.15	3.11	3.05	3.02	3.04	3.01
		15	10.70	2.88	2.86	2.82	2.76	2.77	2.75
		20	14.30	2.72	2.70	2.64	2.60	2.62	2.61
		25	17.87	2.60	2.57	2.53	2.50	2.53	2.50

4.5. Thermal enhancement factor

The study of heat transfer and flow friction characteristics of the artificial roughen duct shows that an enhancement in heat transfer is accompany with friction power penalty due to a corresponding increase in the friction factor. The present CFD study for circular section shows the rough duct with relative roughness pitch (P/e) of 7.14, and relative roughness height (e/D) of 0.042 give the maximum value of average Nusselt number in the order of 2.31 times of smooth duct at higher Reynolds number(18,000). The maximum value of friction factor is found 3.15 times of smooth duct at lower Reynolds number (3800). Hence it is essential to find out the optimal rib dimension and arrangement that will result in maximum enhancement in heat transfer with minimum friction power penalty. A parameter that facilitate simultaneous consideration of thermal and hydraulic performance as defined by Webb and Eckert is given by Eq. (9).

The value of this parameter higher than unity ensures the effectiveness of using an enhancement device and can be use to compare the performance of number of arrangements to decide the best among these. Fig.4.5 shows the variation of the thermal enhancement factor with Reynolds number for all cases for circular section.. It is found that the thermal enhancement factor values vary between 1.1 and 1.72 for the range of parameters investigated. It is observed that roughened duct having circular transverse wire rib with e =1.4 mm and P =15 mm (i.e. P/e=10.70) and (e/D=0.042) gives better thermal enhancement factor for the studied range of Reynolds number. Hence it is recommended that circular transverse wire rib roughened absorber plate with e =1.4 mm and P =15mm.

Finally It is observed that roughened duct having circular rib with e = **1.4** mm and **P = 15** mm (i.e. e/D = **0.042**) gives better thermal enhancement factor (**TEF=1.72**) at a Reynolds number of **15,000**.

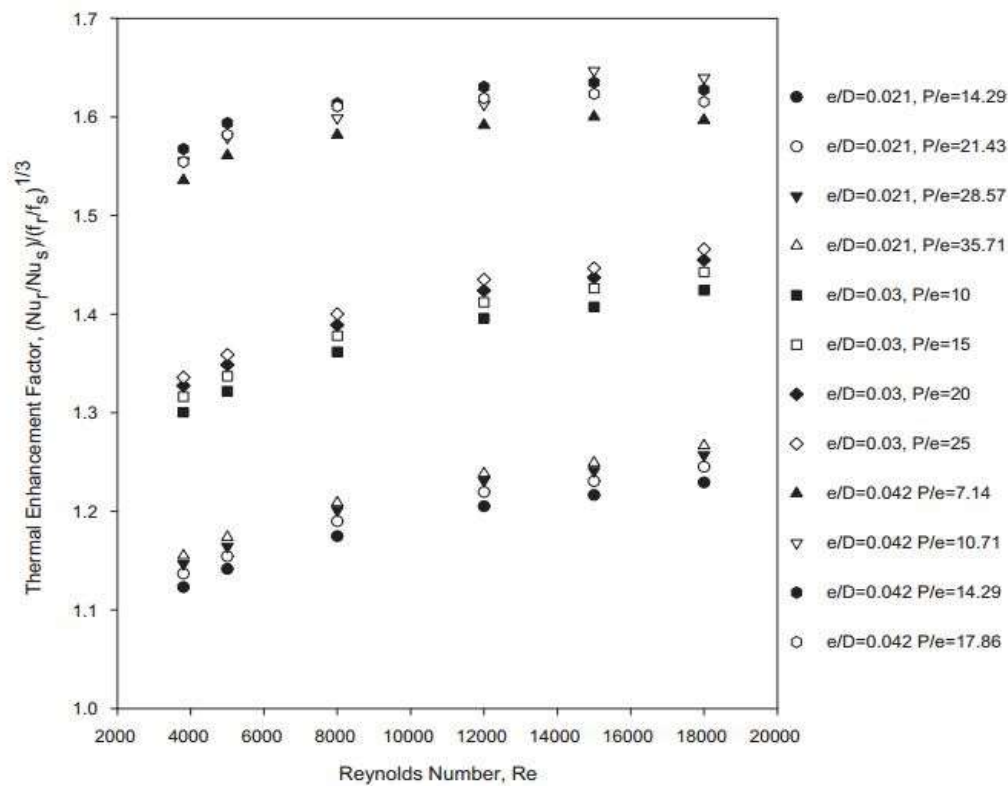


Fig-4.5 Thermal enhancement factor

4.6 Validation of model

In order to validate the present numerical model, the results are compared with available experimental results. Literature search in the area of artificially roughened solar air heater also reveals that the optimum value of relative roughness height generally lies between 0.03-0.047. **Table 4.3** shows the comparison of optimum value of relative roughness height between present CFD simulation and available experimental widely accepted numerical results. On comparison, it has been observed that the optimum value of relative roughness height for present CFD model is found to be 0.045 for circular sectioned rib. The optimum value of relative roughness height from present CFD investigated is found to fall in-between the accepted range i.e. 0.033 and 0.043.

Table:-4.3 Validation model

S. No.	Investigator's	Roughness geometry	Optimum value of relative roughness pitch(p/e)	Optimum value of relative roughness height (e/D)
1	Prasad and Mullick	Transverse wire rib roughness	p/e=12.7	e/D=0.033
2	Prasad and Saini	Transverse wire rib roughness	10	0.020

3	Bhagoria et al.	Transverse wedge shaped rib roughness	7.57	0.033
4	Laurker et al.	Rib-grooved roughness	6	0.036
5	Layek et al.	Chamfered rib-grooved roughness	6	0.04
6	Saini and Saini	Arc shaped rib roughness	10	0.0422
7	Aharwal et al.	Inclined continuous rib roughness with gap	10	0.037
8	Saini and Saini	Dimple- shaped rib roughness	10	0.379
9	Varun et al.	Combination of transverse and inclined rib roughness	8	0.30
10	Bopche and Tandale	Inverted U-shape turbulator	6.67	0.0398
11	Kumar et at.	Discrete W-shaped rib roughness	10	0.0388
12	Hans et al.	Multi V-shaped rib roughness	8	0.043
13	Lanjewar et at.	60 degree V –shaped rib roughness	10	0.0337
14	Singh et at.	Discrete V-down rib roughness	8	0.043
15	Sethi et at	Dimple shaped element arranged in circular fashion	10	0.036
16	Kumar et at.	Multi V-shaped rib roughness with gap	10	0.043
17	AS Yadav and JL Bhagoria	Semi-circular shaped rib roughness	10	0.042
18	AS Yadav and JL Bhagoria	Square- shaped rib roughness	10.71	0.042
19	Karwa and Chitoshiya	V-down discrete rib roughness	10.66	.047

5. CONCLUSION

A 2-dimensional CFD analysis has been carried out to study heat transfer and fluid flow behavior in a rectangular duct of a solar air heater. Basically, we compare the result obtained by with circular transverse wire rib and equilateral triangle transvers wire ribs. The effect of Reynolds number, roughness height, roughness pitch, relative roughness pitch and relative roughness height on the heat transfer coefficient and friction factor have been study. In order to validate the present numerical model, results have been compare with available experimental results under similar flow conditions. CFD Investigation has been carried out in medium Reynolds number flow ($Re=3800-18,000$). The following conclusions are draw from present analysis:

1. The Renormalization-group (RNG) k - ϵ turbulence model predicted very close results to the experimental results. RNG k - ϵ turbulence model has been validated for smooth duct and grid independence test has also been conducted to check the variation with increasing number of cells.
2. Average Nusselt number (Nu) increases with an increase of Reynolds number in all cases for circular ribs. The average Nu tends to decrease when relative roughness pitch (p/e) increases for a fixed value of relative roughness height (e/D) and it also tends to increase when (e/D) increases for a fixed value of (p/e).
3. The maximum value of (Nu) is found to be 117 for circular ribs at (p/e) of 7.14 and (e/D) of 0.042 at a higher Reynolds number, 18,000.
4. The maximum enhancement of average Nusselt number is found to be 2.31 times of smooth duct at (p/e) = 7.14 and relative roughness height (e/D) of 0.042.
5. Average friction factor decreases with an increase of Reynolds number in all cases. The maximum value of average friction factor is found to be 0.0317 for circular ribs at (p/e) of 7.14 and (e/D) = 0.042 at a lower Reynolds number, 3800. The maximum enhancement of average friction factor is found to be 3.15 times of smooth duct at (p/e) = 7.14 and (e/D) = 0.042.
6. The thermal enhancement factor (TEF) values vary between 1.1 and 1.72 for Reynold number 3800-20000. At $P/e = 10.71$ and $e/D = 0.042$ provides better thermal enhancement factor and equal to **1.72** for the studied range of Reynolds number. Finally, we concluded that these parameters is best for deign of solar rough air heater uses in industry purposes.

6 . REFERENCES.

1. Aharwal, K. R., B. K. Gandhi, and J. S. Saini. "Experimental investigation on heat-transfer enhancement due to a gap in an inclined continuous rib arrangement in a rectangular duct of solar air heater." *Renewable energy* 33.4 (2008): 585-596.
2. Han, J. C., and J. S_ Park. "Developing heat transfer in rectangular channels with rib turbulators." *International Journal of Heat and Mass Transfer* 31.1 (1988): 183-195.
3. Tanda, Giovanni. "Effect of rib spacing on heat transfer and friction in a rectangular channel with 45 angled rib turbulators on one/two walls." *International Journal of Heat and Mass Transfer* 54.5 (2011): 1081-1090
4. Kumar, Sharad, and R. P. Saini. "CFD based performance analysis of a solar air heater duct provided with artificial roughness." *Renewable Energy* 34.5 (2009): 1285-1291.
5. Layek, Apurba, J. S. Saini, and S. C. Solanki. "Heat transfer and friction characteristics for artificially roughened ducts with compound turbulators." *International Journal of Heat and Mass Transfer* 50.23 (2007): 4845-4854.
6. Park, J. S., et al. "Heat transfer performance comparisons of five different rectangular channels with parallel angled ribs." *International Journal of Heat and Mass Transfer* 35.11 (1992): 2891-2903.
7. Bhagoria, J. L., J. S. Saini, and S. C. Solanki. "Heat transfer coefficient and friction factor correlations for rectangular solar air heater duct having transverse wedge shaped rib roughness on the absorber plate." *Renewable Energy* 25.3 (2002): 341-369.
8. Saurav, Suman, and V. N. Bartaria. "Heat transfer and thermal efficiency of solar air heater having artificial roughness: a review." *International journal of renewable energy research* 3.3 (2013): 498-508.
9. Luo, Jackson. *Experimental Heat Transfer of Rib Roughened Square, Rectangular and Trapezoidal Cooling Channels*. Northeastern University, 2016.
10. Kumar, Sharad, and R. P. Saini. "CFD based performance analysis of a solar air with artificial roughness." *Renewable Energy* 34.5 (2009): 1285-1291.

- 11.Fouladi, Fama. *Enhancing Convective Heat Transfer over a Surrogate Photovoltaic Panel*. Diss. University of Windsor (Canada), 2017.
- 12.Kumar, Anil, R. P. Saini, and J. S. Saini. "Experimental investigation on heat transfer and fluid flow characteristics of air flow in a rectangular duct with Multi v-shaped rib with gap roughness on the heated plate." *Solar Energy* 86.6 (2012): 1733-1749.
- 13.Yadav, Anil Singh, and Manish Kumar Thapak. "Artificially roughened solar air heater: Experimental investigations." *Renewable and Sustainable Energy Reviews* 36 (2014): 370-411.
- 14.Aharwal, K. R., Bhupendra K. Gandhi, and J. S. Saini. "Heat transfer and friction characteristics of solar air heater ducts having integral inclined discrete ribs on absorber plate." *International Journal of Heat and Mass Transfer* 52.25 (2009): 5970-5977.
- 15.Bopche, Santosh B., and Madhukar S. Tandale. "Experimental investigations on heat transfer and frictional characteristics of a turbulator roughened solar air heater duct." *International Journal of Heat and Mass Transfer* 52.11 (2009): 2834-2848.
- 16.Lanjewar, Atul, J. L. Bhagoria, and R. M. Sarviya. "Heat transfer and friction in solar air heater duct with W-shaped rib roughness on absorber plate." *Energy* 36.7 (2011): 4531-4541.
- 17.Hans, V. S., R. P. Saini, and J. S. Saini. "Heat transfer and friction factor correlations for a solar air heater duct roughened artificially with multiple v-ribs." *Solar Energy* 84.6 (2010): 898-911.
- 18.Kumar, Anil, R. P. Saini, and J. S. Saini. "Heat and fluid flow characteristics of roughened solar air heater ducts—A review." *Renewable Energy* 47 (2012): 77-94.
- 19.Yadav, Anil Singh, and J. L. Bhagoria. "A CFD based thermo-hydraulic performance analysis of an artificially roughened solar air heater having equilateral triangular sectioned rib roughness on the absorber plate." *International Journal of Heat and Mass Transfer* 70 (2014): 1016-1039.
- 20.Manca, Oronzio, Sergio Nardini, and Daniele Ricci. "A numerical study of nanofluid forced convection in ribbed channels." *Applied Thermal Engineering* 37 (2012): 280-292.
- 21.Kumar, Thakur Sanjay, et al. "Use of artificial roughness to enhance heat transfer in solar air heaters-a review." *Journal of Energy in Southern Africa* 21.1 (2010): 35-51.
- 22.Singh, Sukhmeet, et al. "CFD (computational fluid dynamics) investigation on Nusselt n section transverse rib." *Energy* 84 (2015): 509-517.
- 23.Bhushan, Brij, and Ranjit Singh. "A review on methodology of artificial roughness used in duct of solar air heaters." *Energy* 35.1 (2010): 202-212.
- 24.Behura, A. K., Prasad, B. N., & Prasad, L. (2016). Heat transfer, friction factor and thermal performance of three sides artificially roughened solar air heaters. *Solar Energy*, 130, 46-59.
- 25.Prasad, R. K., & Sahu, M. K. (2016). Investigation on optimal thermohydraulic performance of a solar air heater having arc shaped wire rib roughness on absorber plate. *International Journal of Thermodynamics*, 19(4), 214-224
- 26.Jin, Dongxu, et al. "Numerical investigation of heat transfer and fluid flow in a solar air heater duct with multi V-shaped ribs on the absorber plate." *Energy* 89 (2015): 178-190.
27. Rai, Shalini, Prabha Chand, and S. P. Sharma. "An analytical investigations on thermal and thermohydraulic performance of offset finned absorber solar air heater." *Solar Energy* 153 (2017): 25-40.
28. Jin, Dongxu, et al. "Thermohydraulic performance of solar air heater with staggered multiple V-shaped ribs on the absorber plate." *Energy* 127 (2017): 68-77.
29. Thakur DS, Khan MK, Pathak M. Performance evaluation of solar air heater with novel hyperbolic rib geometry. *Renewable Energy*. 2017 May 31;105:786-97.